OCTOBER 01 2005

Measurement of the Doppler shift in forward-scattered waves caused by moderate sea surface motion in shallow waters

Pierre-Philippe J. Beaujean; Guenael T. Strutt

ARLO 6, 250–256 (2005)
https://doi.org/10.1121/1.1989747

Measurement of the Doppler shift in forward-scattered waves caused by moderate sea surface motion in shallow waters

Pierre-Philippe J. Beaujean
Florida Atlantic University, Dept of Ocean Eng., SeaTech Campus, 101 N. Beach Rd, Dania Beach, Florida 33004
pbeaujea@seatech.fau.edu

Guenael T. Strutt
MeshNetworks, Inc., 485 Keller Road, Suite 250, Maitland, Florida 32751-7535
GStrutt@MeshNetworks.com

Abstract: A study of the impulse response of the acoustic channel in shallow waters is presented with respect to space, time, and frequency shift over a time window of two hours. A broadband chirp (42–54 kHz) and a narrow band sine wave (58 kHz) are transmitted from a static source located at 51 and 166 m from a vertical line receiver array. In 20 m of water with 0.4 m of wave height, an average Doppler shift of 20 Hz is measured at 51 m range, and 10 Hz at 166 m range, due to the sea-surface motion.

PACS numbers: 43.30.Gv, 43.30.Re, 43.30.Xm
Date Received: July 27, 2004 **Date Accepted:** July 11, 2005

1. Introduction

Underwater acoustic communications in shallow waters are limited by the combination of time and frequency selective fading caused by the presence of moving boundaries and scatterers. The amount of Doppler shift applied to a propagating wave depends directly on the acoustic path. This phenomenon becomes more significant as the frequency of the transmitted signal increases, which is a serious issue since more bandwidth is available at higher frequencies. A fair amount of research has taken place in modeling and measuring the time spread and Doppler spread present in a signal transmitted horizontally in shallow waters.[1–3] However, the experimental results published mostly focus on low frequencies,[4,5] and provide little detail regarding the spatial distribution of Doppler shift, causing, in turn, Doppler spread.[6,7] The material published regarding high frequencies is usually theoretical.[8] The experimental results published provide limited details regarding the spatial distribution of Doppler shift,[9] or without sufficient angular resolution to separate the individual sources of scattering.[10]

McDaniel[1] provides a theoretical study of the spatial covariance and performance of adaptive beamforming for 30 kHz signals forward scattered from the sea surface. The wind speed varies from 5 to 25 knots, the receiver depth varies from 10 to 320 m, and the range from 300 to 1000 m. The author concludes that both wind speed and geometry strongly impact the horizontal and vertical coherence of these signals. In his study of forward scattering from the sea surface between 15 and 120 kHz, Dahl[8] provides an in-depth comparison between the theoretical and experimental time spread as a function of wind speed and frequency, using omnidirectional sources and a horizontal line receiver array placed in 25 m of water at a distance of 70 to 100 m. Unfortunately, Doppler spread is left aside. Eggen[6,7] uses a recursive least-square approach to identify the scattering function of various shallow and deep water acoustic channels. The study takes place between 15 and 25 kHz, using an omnidirectional source and single channel receiver. The water depth is 15 m and the range varies between 100 m and 5 km. The weather conditions are not provided. A Doppler spread of 2 Hz is observed between the two most dominant ray paths. Kilfoyle[9] provides an estimate of the scattering function, documented by Eggen[11] and measured in the Bahama Islands using a 15 kHz signal with 2.5 kHz of bandwidth. 10 Hz of Doppler spread is observed, but little environmental information is

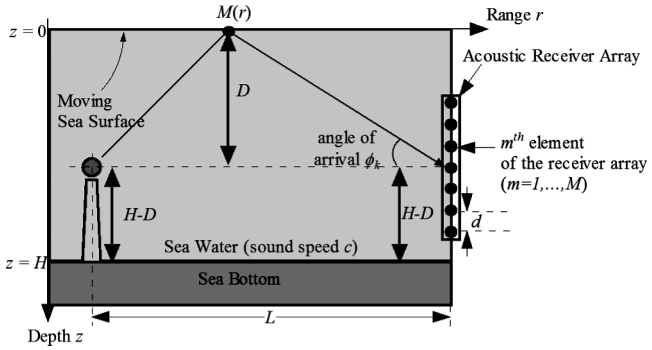

Fig. 1. Experimental setup.

provided. Beaujean[10] observes that, when broadband signals are transmitted between 16 and 32 kHz in 13 m of water and in sea state 2, the product of time spread and Doppler spread varies from 0.001 to 0.1 within minutes, with up to 10 Hz of Doppler spread. Unfortunately, the distance between the source and the receiver is 3.2 km, which greatly limits the angular separation of the multipath.

If a vertical receiver array of sufficient angular resolution records a combination of broadband and narrow band signals transmitted from a static source, it is possible to identify the paths subject to different Doppler shifts, using conventional beamforming and frequency analysis. In this article we provide the detailed steps of such an approach, followed by an experimental evaluation of the angular distribution of time delay and Doppler shift for a signal transmitted between 42 and 58 kHz.

2. Scientific background

The determination of the Doppler shift caused by surface motion is the main focus of this work. A specific acoustic signal is transmitted from a static point source located at distance L from a vertical receiver array (Fig. 1). The source and center of the receiver array are at equal depth D. The water depth H and sound velocity c are constant. The surface and bottom roughness are assumed to be small, so that the acoustic energy incident to either boundary is mostly scattered forward. Each point $M(r)$ of the sea surface has a specific particle velocity causing Doppler shift of the scattered waves. Two waveforms are transmitted simultaneously in separate frequency bands: (i) a narrow band 100 ms sine wavecentered at 58 kHz, subject to small Doppler shifts measured with an auto-regressive (AR) estimation of the signal Power Spectral Density (PSD). (ii) A broadband 100 ms chirp centered at 48 kHz, with 12 kHz of bandwidth (−20 dB), used to compute the in-band impulse response of the acoustic channel for various angles of arrival.

A. Beamforming

The angular distribution of the channel response between 42 and 54 kHz is estimated using delay-line beamforming of the broadband pulse, centered at f_{broad} Hz and recorded on each channel of the receiver array. The complex matched-filter[12] outputs of the recorded signals are represented as a matrix $[\tilde{x}_{\text{chirp}}(t)]$ of M channels by N time samples. The beamformed signal array $[\tilde{y}_{\text{chirp}}(t)]$ is obtained by multiplying the Hamiltonian of $[H_{\text{broad}}]$ with $[\tilde{x}_{\text{chirp}}(t)]$,

$$[\tilde{y}_{\text{chirp}}(t)]=[H_{\text{broad}}]^H[\tilde{x}_{\text{chirp}}(t)], \tag{1}$$

$$H_{\text{broad}}(\phi_k,m)=g_m e^{j2\pi f_{\text{broad}}\, md\, \sin(\phi_k)/c}. \tag{2}$$

d is the spacing between each hydrophone. g_m is the mth array shading coefficient, obtained from

a Kaiser window. The angular distribution of the narrow band signal, centered at f_{narrow} Hz, is obtained using the same beamforming technique. In the base band, the complex received signal array is $[\tilde{r}_{\text{narrow}}(t)]$, and the beamformed signal array $[\tilde{y}_{\text{narrow}}(t)]$ is

$$[\tilde{y}_{\text{narrow}}(t)]=[H_{\text{narrow}}]^H[\tilde{r}_{\text{narrow}}(t)], \tag{3}$$

$$H_{\text{narrow}}(\phi_k,m)=g_m e^{j2\pi f_{\text{narrow}} md\sin(\phi_k)/c}. \tag{4}$$

B. Auto-regressive estimation of the signal PSD

The PSD of each beamformed narrow band signal is computed to determine the amount of Doppler shift present in this signal. AR PSD estimation is selected to achieve sufficient frequency resolution. For each direction of arrival, an AR filter of order p is computed. If y_i represent the ith time sample of the kth row of $[\tilde{y}_{\text{narrow}}(t)]$, the AR estimate $\hat{y}_i$ of y_i is

$$\hat{y}_i=\sum_{l=2}^{p+1} b_l y_{i-(l-1)}. \tag{5}$$

The vector $\{b\}$ can be determined from the autocorrelation function[12]

$$\{b\}=\begin{bmatrix} R_{yy}(0) & \cdots & R_{yy}(-p+1) \\ \vdots & \ddots & \vdots \\ R_{yy}(p-1) & \cdots & R_{yy}(0) \end{bmatrix}^{-1}\begin{Bmatrix} R_{yy}(1) \\ \vdots \\ R_{yy}(p) \end{Bmatrix}. \tag{6}$$

The resolution of the AR spectral estimator can be assessed by determining the minimum frequency separation between two distinct sinusoids embedded in white noise:[13]

$$\delta f_{AR}=1.03/(p[\eta(p+1)]^{0.31}), \tag{7}$$

where η is the signal-to-noise ratio (SNR) of the narrow band signal. The filter order p is selected to minimize the Akaike Information Criterion.[13]

C. Echo identification and determination of the wave characteristics

Consider the experimental setup shown in Fig. 1. The theoretical time delay, measured at the center of the receiver array, between the direct echo ($\phi_{k_1}=0$) and the echo arriving at ϕ_k, is

$$\Delta\tau_k=\frac{1}{c}\left[\frac{D}{\sin\phi_k}+\sqrt{(L-D\cot\phi_k)^2+D^2}-L\right]. \tag{8}$$

The sea surface is modeled as a horizontal plane of peak vertical velocity $U_{\max}$, causing a Doppler shift Δf_k to the narrow band signal. If both the source and receiver are static,

$$U_{\max}=\frac{c\Delta f_k}{f_{\text{narrow}}\sin(\phi_k)}. \tag{9}$$

If the wave height is significantly smaller than the water depth, the surface wavelength λ_{wave} can be determined using gravity waves theory. If $g=9.81$ m/s^2 is the constant of gravity,

$$\lambda_{\text{wave}}=2\pi g\left(\frac{H}{2U_{\max}}\right)^2. \tag{10}$$

3. Experimental results

The experiment, described in Fig. 1, was set up to evaluate *in situ* the impact of surface motion on the frequency spectrum of a sound probe. Table 1 provides a summary of the experimental

Table. 1. Environmental parameters.

Environmental parameters at the first receiver location			
Distance	51 m	Speed of sound	1535 m/s
Direct time delay	33.25 ms	Wave height	0.4 m
Depth	20 m	Wind speed	4 m/s
Source and array depth	18 m	SNR	61.4 dB
Environmental parameters at the second receiver location			
Distance	166 m	Speed of sound	1535 m/s
Direct time delay	108.10 ms	Wave height	0.4 m
Depth	20 m	Wind speed	4 m/s
Source and array depth	18 m	SNR	49.3 dB

conditions. The length of the surface waves varied between 2 and 3 m. Data were collected at a distance of 51 and 166 m (measured with DPGS) from the source. This distance was kept short to maximize the SNR and the angular separation between acoustic paths. The equipment was deployed on a sandy seabed, 1800 m east of Port Everglades, Florida. The source emitted sound within $\pm 60°$ at -3 dB in the vertical plane and was omnidirectional in the horizontal plane, with a source level of 175 dB *re* 1 μPa at 1 m. The linear receiver array consisted of $M=64$ hydrophones spaced $d=7.5$ mm apart. Each channel was sampled at 1 MHz, digitally filtered between 40 and 60 kHz and decimated into the baseband.[13]

A. Study of the data collected at 51 m range

Figures 2(a) to 2(c) show the channel response measured between 42 and 56 kHz as a function of the angle of arrival at 5 min intervals. The source is located at 51 m from the receiver. The main lobe of the array beampattern has a beamwidth of 2° at -3 dB. The array shading coefficient of the Kaiser window is $\beta=3$. The direct path is observed within the first millisecond of the record, between $-2°$ and 2°. From Table 1 and (8), the path bouncing off the sea surface at midrange ($L/2$) must arrive 7.5 ms after the direct path at an angle of 35.2°, while the midrange bottom

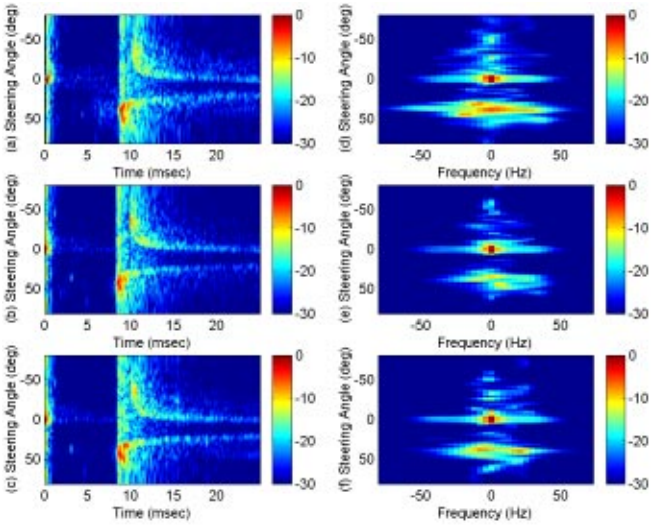

Fig. 2. Sequence of three measurements taken at range $L=51$ m and at 5 min intervals. (a) to (c) Normalized envelope of the matched-filtered broadband signal (dB); (d) to (f) Normalized AR PSD estimation of the narrow band signal (dB).

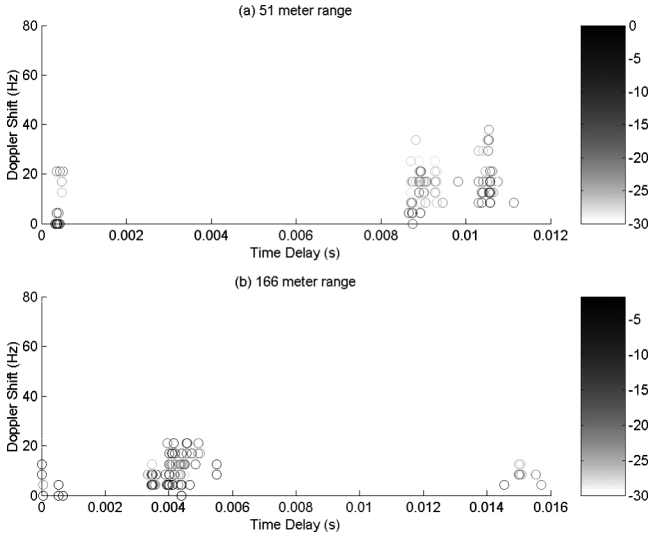

Fig. 3. Peak magnitude of the narrow band signal versus Doppler shift and time delay measured (a) across all three records at $L=51$ m and (b) across all three records at $L=166$ m.

path must arrive 0.1 ms after the direct path at an angle of $-4.5°$. For each measurement, a surface echo is observed 8 to 9 ms after the direct path at an angle of 35° to 40°. The bottom echo is received less than 1 ms after the direct path between $-6°$ and $-4°$.

Figures 2(d) to 2(f) show the PSD of the 58 kHz sine wave as a function of the angle of arrival and frequency shift $\Delta f=f-f_{\text{narrow}}$. $N=9500$ data points (237.5 ms) are processed per array channel. Here $\eta=61.4$ dB, $p=200$ taps so that $\delta f_{\text{AR}}=12$ μHz. Each row in Fig. 2 corresponds to an individual signal transmission. The PSD level is at a maximum between $-2°$ to 2°, which corresponds to the direct path. No Doppler shift is observed in this direction since both the source and receiver are static. The bottom echo is observed between 4° and 6°. No Doppler shift is observed in the bottom echo, indicating that the sandy bottom is still. A significant PSD level is also observed between 35° and 40°, which corresponds to the surface bounce at mid range. The Doppler shift measured in this direction varies between 10 Hz in Fig. 2(e) and 40 Hz in Fig. 2(d). Since the transmitted signal has 10 Hz of bandwidth, the direct echo and surface echo may be totally incoherent, while the direct echo and bottom echo remain coherent at all times.

Figure 3(a) shows the PSD level of the narrow band signal as a function of the absolute frequency shift $|\Delta f|=|f-f_{\text{narrow}}|$ and time of arrival, obtained from the broadband measurements shown in Figs. 2(a) to 2(c). As expected, the midrange surface echoes form a clutter 8.5 to 9.5 ms after the direct path, with up to 40 Hz of Doppler shift. The centroid of this clutter is centered at 9 ms delay and 20 Hz of Doppler shift. Since the SNR is very high, the only possible cause of fluctuation of the time delay and Doppler shift is the motion of the sea surface. Using Table 1, Eqs. (8), (9), and (10) and the delay and Doppler shift measured at the centroid, we obtain the environmental parameters $L=44$ m, $U_{\max}=0.92$ m/s, and $\lambda_{\text{wave}}=2.9$m. An error in position estimation of 7 m is realistic, as both the source and receiver are placed using DGPS, with an error circle of 5 m. The wavelength measurement falls within the observed range (2 to 3 m), although the precision of this estimate cannot be checked against other accurate measurements.

B. Study of the data collected at 166 m range

Figures 4(a) to 4(c) show the channel response measured between 42 and 56 kHz as a function of the angle of arrival at 5 min intervals. The source is located 166 m from the receiver. The data

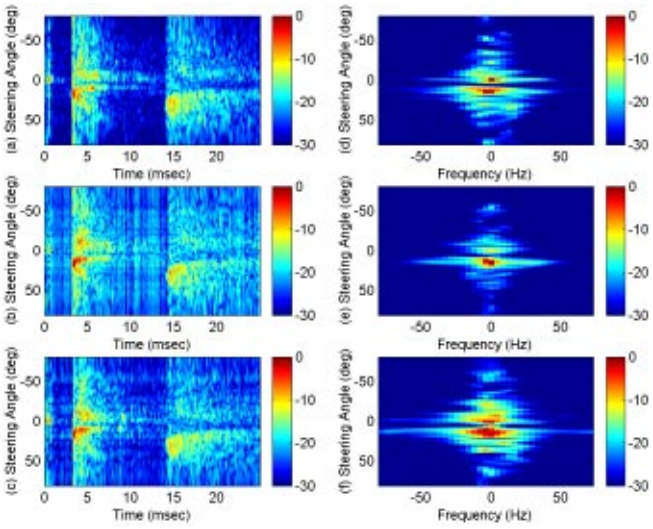

Fig. 4. Sequence of three measurements taken at range $L=166$ m and at 5 min intervals. (a) to (c) Normalized envelope of the matched-filtered broadband signal (dB). (d) to (f) Normalized AR PSD estimation of the narrow band signal (dB).

have been collected 90 min after the experiment at 51 m. The direct path is observed after one millisecond, between $-2°$ and $2°$. Using Table 1 and (8), the midrange surface path must arrive 2.5 ms after the direct path at an angle of 12.2°, while the midrange bottom path must arrive 0.03 ms after the direct path at an angle of $-1.4°$. For each received signal, a surface echo is observed 3 to 4 ms after the direct path at an angle of 10° to 15°. The bottom echo cannot be separated from the direct echo due to lack of time and angular resolution.

Figures 4(d) to 4(f) show the PSD of the 58 kHz sine wave as a function of the angle of arrival and frequency shift. The same number of samples and taps is used at 51 and 166 m range. The SNR is $\eta=49.3$ dB and $p=200$ taps so that $\delta f_{AR}=29$ μHz. The PSD level is at a maximum between $-2°$ to $2°$, which corresponds to the combination of direct and bottom paths. No Doppler shift is observed in this direction since the source, receiver, and sea bottom are static. A high PSD level is observed between 10° to 15°, which corresponds to the surface bounce at midrange. The Doppler shift measured in this direction fluctuates between 5 Hz in Fig. 4(e) and 20 Hz in Fig. 4(f). These Doppler shifts are lower than the ones observed at a 51 m range, which is to be expected since the signal bounces off the surface at a much smaller grazing angle. The lower Doppler shift also indicates that surface echo and direct echo keep some level of coherence as the ratio of range over depth increases. Figure 3(b) shows the PSD level of the narrow band signal as a function of absolute frequency shift and time of arrival, obtained from the broadband measurements shown in Figs. 4(a) to 4(c). The midrange surface echoes form a clutter between 3 and 5 ms after the direct path, with up to 20 Hz of Doppler shift. The centroid of this clutter is centered at 3 ms from the direct path and 10 Hz of Doppler shift. Using Table 1, Eqs. (8), (9) and (10), we obtain $L=143$ m, $U_{max}=1.1$ m/s, and $\lambda_{wave}=2.1$ m. The error in the position estimation of 23 m is excessive, and is attributed to the sensitivity of Eq. (8) to angle fluctuations when the angle of arrival is small. As in the first experiment, the wavelength measurement falls within the observed interval of 2 to 3 m.

4. Conclusion

Despite the short observation time, the experiment described in this article leads to several important observations. First, the observed and modeled experimental conditions match quite accurately, which confirms the good quality of the data recorded. Second, the Doppler shift

measured at 51 m is twice the tone bandwidth, which indicates that the direct echo and surface echo are partly or totally incoherent and could be separated using very narrow band filters. Finally, the individual paths are more easily identified and separated at a shorter range, while the Doppler shift caused by the sea surface increases as the range decreases. As the range increases to 166 m, the Doppler shift and angular separation of the paths decreases, indicating that more coherent signal interferences between the direct path and the surface path are to be expected.

Acknowledgments

This work has been sponsored by the Office of Naval Research, Dr. Tom Curtin.

References and Links

[1] S. T. McDaniel, "Spatial covariance and adaptive beamforming of high-frequency acoustic signals forward scattered from the sea surface," IEEE J. Ocean. Eng. **16**, 415–419 (1991).
[2] G. V. Norton and J. C. Novarini, "The effect of sea-surface roughness on shallow water waveguide propagation: A coherent approach," J. Acoust. Soc. Am. **99**, 2013–2021 (1996).
[3] D. R. Dowling and D. R. Jackson, "Coherence of acoustic scattering from a dynamic rough surface," J. Acoust. Soc. Am. **93**, 3149–3157 (1993).
[4] H DeFerrari, N. Williams, and H. Nguyen, "Focused arrivals in shallow water propagation in the straits of Florida," ARLO **4**, 106–111 (2003).
[5] M. V. Brown and G. V. Frisk, "Frequency smearing of sound forward-scattered from the ocean surface," J. Acoust. Soc. Am. **55**, 744–749 (1974).
[6] T. H. Eggen, A. B. Baggeroer, and J. C. Preisig, "Communication over doppler spread channels—Part I: Channel and receiver presentation," IEEE J. Ocean. Eng. **25**, 62–71 (2000).
[7] T. H. Eggen, A. B. Baggeroer, and J. C. Preisig, "Communication over Doppler spread channels—II: Receiver characterization and practical results," IEEE J. Ocean. Eng. **26**, 612–621 (2001).
[8] P. H. Dahl, "High-frequency forward scattering from the sea surface: The characteristic scales of time and angle spreading," IEEE J. Ocean. Eng. **26**, 141–151 (2001).
[9] D. B. Kilfoyle and A. B. Baggeroer, "The state of the art in underwater acoustic telemetry," IEEE J. Ocean. Eng. **25**, 4–27 (2000).
[10] P.-P. J. Beaujean and L. R. LeBlanc, "Adaptive array processing for high-speed acoustic communication in shallow water," IEEE J. Ocean. Eng. **29**, 807–823 (2004).
[11] T. H. Eggen, "Underwater acoustic communication over Doppler spread channels," Ph.D. thesis, Massachusetts Institute of Technology, 1997.
[12] S. M. Kay, *Modern Spectral Analysis, Theory and Application* (Prentice–Hall, Englewood Cliffs, NJ, 1988).
[13] G. T. Strutt, "The effect of sea surface motion on underwater acoustic communication systems," M.S. thesis, Florida Atlantic University, Boca Raton, FL, 1999).